ACS OMEGA

http://pubs.acs.org/journal/acsodf

Article

# Effect of Temperature on the Diffusion and Sorption of Cations in Clay Vermiculite

Cailun Wang,* Vyacheslav Fedorovich Myshkin, Valeriy Alekseevich Khan, Andrew Dmitrievich Poberezhnikov, and Alexander Petrovich Baraban

Cite This: *ACS Omega* 2022, 7, 11596−11605

Read Online

ACCESS | Metrics & More | Article Recommendations

**ABSTRACT:** The MD method for modeling vermiculite containing $Na^+$, $Rb^+$, $Cs^+$, $Mg^{2+}$, and $Ba^{2+}$ cations shows the following: With a weak swelling of clay, the temperature has no significant effect on the diffusion of water and cations through vermiculite. With a high content of water in vermiculite, the effect of temperature on the diffusion coefficient of water is greater than that of cations. We studied the structure of RDF ions in $Na^+$-vermiculite, in which some of the cations are replaced by $Rb^+$, $Cs^+$, $Mg^{2+}$, and $Ba^{2+}$. Cations of alkali and alkaline earth metals compete with $Na^+$ ions for adsorption sites on the surface of the clay layer. The alkaline earth metal cations are in the middle between the clay layers due to their higher charge and stronger hydration. In this case, $Na^+$ is localized at the surface of the clay layer. Thus, cations of alkaline earth metals have little effect on the temperature dependence of the diffusion coefficient $Na^+$.

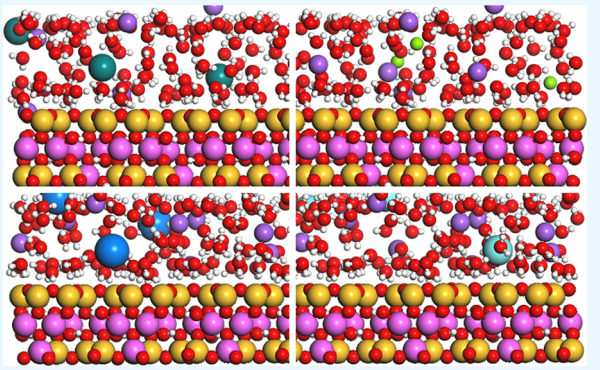

## 1. INTRODUCTION

Clay, a mineral widespread on earth, is used in many fields. Clays have a very low hydraulic conductivity and a high ability to retain cations and inhibit the diffusion of cations.[1,2] These properties are associated with the patterns of water absorption, which determine the swelling.[2−8] Nowadays, clay has become a recognized material as an engineering safety barrier for radioactive waste disposal.[9−12]

It is known that the temperature of the surface layers of earth increases with depth. Radioactive decay also leads to the heating of the substance. Therefore, in recent years, many scientists have studied the effect of elevated temperatures of deep geological reservoirs on the processes of interaction between clay and various cations, including radioactive ones.[13−23] Temperature affects different processes in different ways. For example, as the temperature decreases, the distribution of interlayer water tends to be more uniform.[24] In this case, the diffusion coefficients of water and cations increase with increasing temperature. It is known that temperature has a stronger effect on water molecules.[25] However, the temperature dependence of the barrier properties of clay minerals has not been sufficiently studied.

Vermiculite is a layered clay mineral with a 2:1 structure consisting of an alumina (octahedral) sheet sandwiched between two tetrahedral silicon sheets. Isomorphic substitution of silicon for aluminum in the tetrahedral position leads to the appearance of a negative charge on the surface of the clay layer. Equilibrium is achieved through checks and balances between water molecules and cations between the clay layers. As a result, a layered crystal structure is formed.[24] Therefore, the diffusion rate of interlayer cations strongly depends on the content of water molecules in the interlayer space (or is associated with the properties of clay swelling). In humid conditions, interlayer cations can interact with water molecules, forming various complexes depending on their charge and ionic radius. These processes significantly affect the amount of water between layers and the distance between layers of clay.[26]

Clay minerals do not have long-range order due to the small size of the sheet and the peculiarities of their packing, which make it difficult to accurately characterize minerals by experimental methods. Experimental XRD and NMR methods are available to study the effect of cation size and charge on the distances between the basal planes of clay layers.[27] However, it is difficult to experimentally determine the structure of molecular bonds between clay layers and their kinetic behavior. It is also difficult to experimentally measure the porosity of clay

Received: October 29, 2021
Accepted: March 21, 2022
Published: March 30, 2022

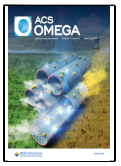





https://doi.org/10.1021/acsomega.1c06059
*ACS Omega* 2022, 7, 11596−11605

and changes in the nature (type) of interaction between ions and water molecules located between the layers.

The advantages of molecular dynamics (MD) modeling are associated with the ability to describe processes at the atomic level and thermodynamic properties. With ab initio MD, you can calculate the details of the molecular structure (bond lengths, bond angles, and forces). Therefore, molecular modeling is an excellent way to gain an understanding of the molecular structure and dynamics of clay minerals at the atomic level.

The size and charge of interlayer cations in clay minerals play an important role in their swelling.[28,29] It was also suggested that the number and spatial arrangement of negative charges are the main factors that determine the degree of hydration and that they determine the number of water molecules in the interlayer space of the mineral.[30] For example, when some Si atoms are replaced by Al atoms, the centers of negative charges can be located in octahedral and tetrahedral sheets. In this case, the charges can be distributed evenly or form clusters.

Most of the research, however, has focused on one type of cation in pure clay.[1,4,5,31−33] The charge-balancing ions in natural clays are usually small inorganic cations such as $Na^+$ or $K^+$ but can be replaced with more complex ions. Different types of cations react differently to temperature changes. For example, the adsorption of $Pb^{2+}$ on bentonite decreases with increasing temperature;[34] at higher temperatures, the adsorption of $Cu^{2+}$ on bentonite[22] and $Th^{4+}$ on illite[35] is more favorable. Some metal ions (for example, Zn and Cd) are very sensitive to temperature changes, and their effective diffusion coefficient increases 10-fold with increasing temperature in the range from 290 to 330 K[13]. Some cations (for example, $Li^+$, $Na^+$, $Cs^+$, $Ca^{2+}$, and $Sr^{2+}$) show a significant increase in the diffusion rate with increasing temperature.[4,23,31] In this case, the addition of ions of small radius between the layers of montmorillonite clay decreases the distance between them,[7] which in turn reduces the diffusion coefficient of interlayer cations.[2] At temperatures above 423 K, this can lead to a decrease in the layer's charge and some of the interlayer cations can migrate to the octahedral position of the silicate layer, neutralizing the negative charge located there (the Hoffmann−Clemen effect).[36,37] It is noted that heating can even cause the penetration of all cations into the clay layers. Therefore, the clay layers are in direct contact with each other at temperatures above 473 K.[38]

In this study, the effect of temperature changes, in the range of 275−425 K, on the diffusion of several ions between clay layers was studied. This made it possible to detect the corresponding changes in the diffusion properties of water molecules and cations in swollen clays under the influence of temperature. The experimental study of the dynamics of ions and water in macroscopic clay samples is complicated by the presence of numerous pores in the system (between clay aggregates, clay particles, and layers of clay mineral = clay layers). Therefore, we used the method of microscopic modeling based on Newtonian mechanics, modeling of molecular dynamics, in modeling the process of molecular motion to obtain static and dynamic information about ions by changing the distance between clay layers. The effects of temperature and the presence of various cations of alkali and alkaline earth metals ($Rb^+$, $Cs^+$, $Mg^{2+}$, and $Ba^{2+}$) on the diffusion of water and $Na^+$ ions in clay were studied.

## 2. SIMULATION DETAIL

Modeling was carried out using the Materials Studio 7.0 software. The clay model was based on the structure obtained by Wyckoff[39] for dioctahedral vermiculite modeling for the $C2/C$ space group.[40] Geometric dimensions of the model are $20.9342 \times 27.2596$ Å$^2$ and angles $\alpha = \gamma = 90°$ and $\beta = 95.64°$, which correspond to 12 calculated cells in a vermiculite layer. In a tetragonal vermiculite sheet, some of the Si atoms are replaced by Al. Therefore, the total surface charge of the vermiculite layer is −1 e per unit cell. The calculated cell incorporated a total of 1842, forming 286 water molecules, 2 clay layers, and 2 interlayer regions.

The regularity of the arrangement of charges over the surface of the layers affects the diffusion coefficient. To determine the dependence of the diffusion coefficient on temperature, one of the types of charge distribution was used only on one surface of the layer. In this case, the molecular layer is negatively charged, due to which cations are attracted to it. The negative charge in clay layers is compensated by interlayer $Na^+$ counterions. With partial replacement of $Na^+$ counterions on ions $Cs^+$, $Rb^+$, $Mg^{2+}$, and $Ba^{2+}$, the unit cell of vermiculite can be represented as $Na_{0.75}(Cs/Rb)_{0.25}(Si_7Al_5O_{20}(OH)_4)$ or $Na_{0.66}(Mg/Ba)_{0.33}(Si_7Al_5O_{20}(OH)_4)$. Before the calculations, the cations were randomly placed between the clay layers. To obtain a large complex system of clay minerals obeying periodic boundary conditions in all three spatial directions, the original cell is replicated to form a supercell. Skipper et al.[41] showed that the properties of a relatively small simulated cell still represent a macroscopic system unaffected by the artificial long-range symmetry of the periodic lattice used. According to the data of the study,[42,43] at the distance between the layers of clay of 17.5 Å, a three-layer structure of water molecules is formed in this volume. Therefore, in the calculations, this distance was used. The structure of the computational cell is shown in Figure 1.

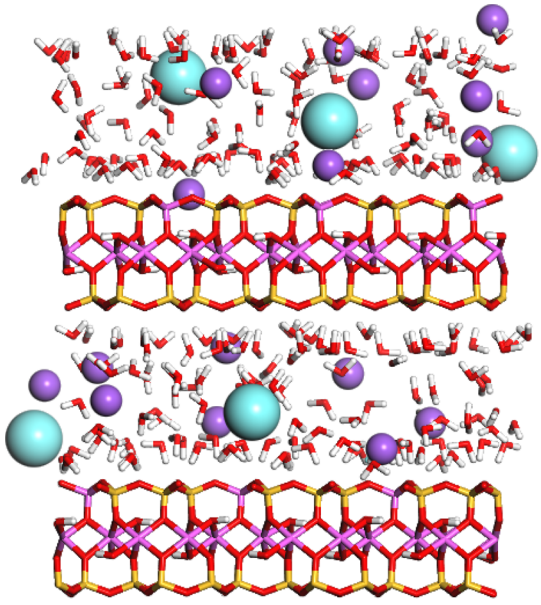

**Figure 1.** Projection of a vermiculite crystal saturated with water onto a plane perpendicular to the basal surface of the layer. Oxygen, red; Al, pink; Si, yellow; and H, gray. Large spheres between layers, free cations: Na, violet and Cs, blue.



https://doi.org/10.1021/acsomega.1c06059
ACS Omega 2022, 7, 11596−11605

The model of interaction between vermiculite and water molecules modeled in this study uses the force field ClayFF.[25] Many studies have shown that the ClayFF force field is very effective in modeling the structure of hydroxide and clay minerals, as well as the interaction of aqueous solutions and solvents with the surfaces of minerals.[44] The total energy in molecular dynamics modeling is based on the interaction of individual atoms in the system, i.e., Coulomb interaction, van der Waals interaction, and bond angle interaction.

$$E^{\text{total}} = E^{\text{bond-stretch}} + E^{\text{angle-bend}} + E^{\text{Coulomb}} + E^{\text{VDW}} \quad (1)$$

where $E^{\text{VDW}}$ is the van der Waals interaction energy.

The van der Waals interaction between molecules is described by the Lennard–Jones (L–J) potential model. The total potential energy of the system is the sum of all interacting positions

$$U = \sum_i \sum_j \left\{ \frac{q_i q_j}{r_{ij}} + 4\varepsilon_{ij} \left[ \left( \frac{\sigma_{ij}}{r_{ij}} \right)^{12} - \left( \frac{\sigma_{ij}}{r_{ij}} \right)^{6} \right] \right\} \quad (2)$$

where $r_{ij}$ is the distance between atoms $i$ and $j$, $q_i$ and $q_j$ are charges of atoms $i$ and $j$, and $\sigma$ and $\varepsilon$ are the parameters of the Lennard–Jones interaction potential.

Lennard–Jones potentials are associated with combinations of parameters of various ionic interactions and have the following form:

$$\sigma_{ij} = (\sigma_i + \sigma_j) : 2 \quad (3)$$

$$\varepsilon_{ij} = \sqrt{\varepsilon_i \varepsilon_j} \quad (4)$$

The atomic charges and Lennard–Jones potential parameters assigned to each atom in the calculated clay cell are taken from the ClayFF force field.[25] This force field more realistically represents the local charge inhomogeneity that forms around each specific area of replacement in the clay layer. The ClayFF force field, consisting of nonbonding members (electrostatic and van der Waals), predicts the structural and dynamic properties of the clay in good agreement with the experiment.[45−47] Water molecules are represented by a simple point charge (SPC) model with flexible intramolecular interactions. The potential parameters and atomic charge of the clay mineral are given in Table 1. Electrostatic interactions under periodic boundary conditions are considered by the Ewald summation method.

When simulating using the Materials Studio code, a local energy minimum was initially determined for each system, which was achieved in less than 5000 calculation steps. Clay temperature was set in the range of 275–425 K with an interval of 25 K. For the simulation, NPT was preliminarily used for a calculation time of 20 ps with a step of 0.1 fs. The results were obtained using an ensemble NVT with a given system equilibrium of 1000 ps and numerical integration of the equations of motion of atoms with a time step of 1 fs. The temperature control method was a Nosé–Hoover thermostat. This ensured that the temperature of the system was controlled with the required accuracy. Every 500 steps, the calculated data of the self-diffusion coefficients of water molecules and counterions were saved.

## 3. RESULTS AND DISCUSSION

**3.1. Diffusion of Interlayer Particles.** Ions of different elements can be simultaneously located between the molecular layers of a natural clay mineral. We used Na-vermiculite, which contains $Na^+$ between the clay layers. In this case, part of the interlayer sodium ions was replaced by $Cs^+$ and $Rb^+$ ions, which have an equivalent charge. Molecular dynamics modeling was carried out under the condition that the clay density remained constant. The effect of various ions on the self-diffusion of interlayer cations was studied. The self-diffusion coefficients for cations and water molecules in the interlayer space were calculated on long time scales using the Einstein relation for the case with two dimensions:

$$D = \frac{1}{4} \cdot \frac{d}{dt} \langle (R(t) - R(0))^2 \rangle \quad (5)$$

where $R(0)$ is the initial position of the particle and $R(t)$ is the position of the particle in $t$ time.

The temperature dependence of the self-diffusion coefficients of various ions between the layers of the mineral has been insufficiently studied. The diffusion coefficients of water molecules calculated by us in different types of vermiculite are shown in Figure 2. In the temperature range of 275–425 K, the diffusion coefficient of water molecules increases nonlinearly with increasing temperature. It can be seen that the addition of the second cation decreases the diffusion coefficient of water molecules at similar levels of hydration. Highly charged cations have a greater effect on the diffusion rate of water molecules.

The graphs in Figure 2 can be explained as follows: Molecules and atoms in liquids and solids are in potential wells

**Table 1. Lennard-Jones Parameters Used in Vermiculite with ClayFF Force**

| layer | element | $q$ (e) | $R$ (Å) | $\varepsilon$ (kcal mol$^{-1}$) | ref |
|---|---|---|---|---|---|
| water | O | −0.8200 | 3.5532 | 0.1554 | 25 |
| | H | 0.4100 | 4.5775 | | 25 |
| tetrahedral | O | −1.1688 | 3.5532 | 0.1554 | 25 |
| | Si | 2.1000 | 3.7064 | $1.8405 \times 10^{-6}$ | 25 |
| | Al | 1.5750 | 3.7064 | $1.8405 \times 10^{-6}$ | 25 |
| octahedral | O | −1.1808 | 3.5532 | 0.1554 | 25 |
| | H | 0.4250 | 4.5775 | | 25 |
| | Al | 1.5750 | 4.7943 | $1.3298 \times 10^{-6}$ | 25 |
| cation | $Na^+$ | 1.0 | 2.6378 | 0.1301 | 25 |
| | $Cs^+$ | 1.0 | 4.3002 | 0.1000 | 25 |
| | $Rb^{2+}$ | 2.0 | 4.114 | 0.04 | 23 |
| | $Ba^{2+}$ | 2.0 | 4.2840 | 0.0470 | 25 |
| | $Mg^{2+}$ | 2.0 | 1.6444 | 0.87557 | 48 |

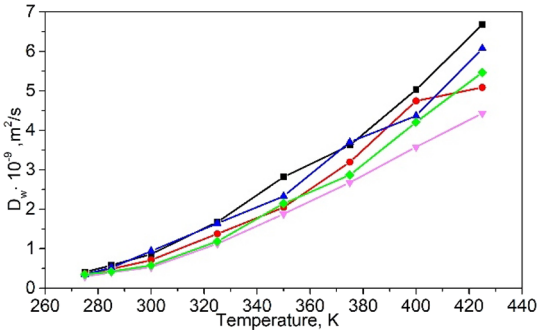


**Figure 2.** Variation of self-diffusion coefficient of water with temperature in vermiculite containing different kinds of interlayer counterions: Na-Ver (black), Na/Rb-Ver (red), Na/Cs-Ver (blue), Na/Mg-Ver (pink), and Na/Ba-Ver (green).



https://doi.org/10.1021/acsomega.1c06059
ACS Omega 2022, 7, 11596−11605

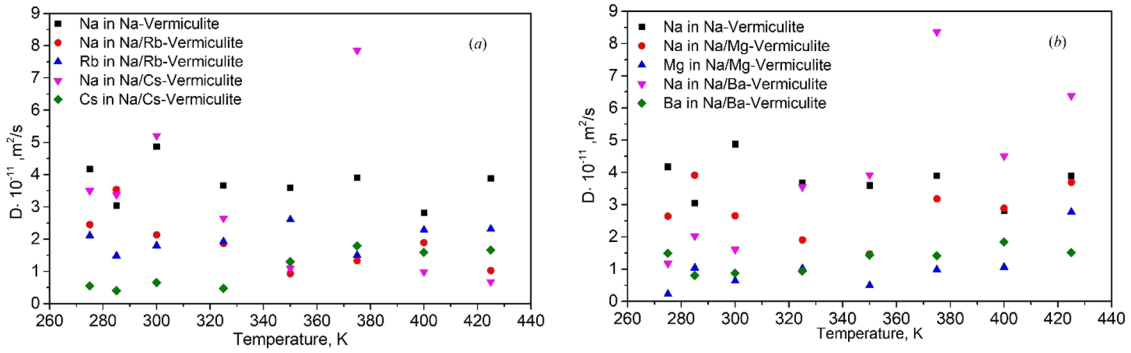


**Figure 3.** Temperature dependence of the self-diffusion coefficient of cations in vermiculite containing several interlayer counterions: (a) alkali and (b) alkaline earth metals.

due to the limiting influence of neighboring particles. In this case, diffusion is associated with a change in the spatial position of particles and their thermal velocity. Exit from one potential well and transition to another are possible due to fluctuations in the energy of thermal vibrations. The time required for the appearance of fluctuations in the energy of thermal vibrations of atoms or molecules, exceeding the depth of the potential well, can be determined from the Frenkel equation, as follows:

$$t = \tau_0 \exp\left(\frac{\Delta E_n}{kT}\right) \quad (6)$$

where $\tau_0 = 10^{-13}-10^{-12}$ s is the period of vibration of an atom in a solid at a given temperature, $\Delta E_n$ is the energy fluctuation magnitude, $k$ is the Boltzmann's constant, and $T$ is the temperature.

With an increase in temperature, the appearance time of a given fluctuation of the thermal vibration energy decreases nonlinearly, increasing the diffusion rate. In this case, in accordance with eqs 5 and 6, an exponential dependence of the diffusion coefficient of water molecules on temperature is observed.

However, for mixtures of Na with monovalent ions, small fluctuations are observed with respect to the values described by the exponential function. The most likely reason for this is a change in the number of water molecules in the hydration shell of the cation. This changes the ratio of water molecules trapped in ion−dipole and hydrogen bonds. Therefore, the average value of the depth of the potential well for water molecules changes nonmonotonically.

The temperature dependence of the diffusion coefficients of water in a mixture with different cations observed in Figure 2 can be explained as follows. Ionic radii are 0.95 Å for $Na^+$, 1.48 Å for $Rb^+$, and 1.69 Å for $Cs^+$. Larger cations have a greater screening effect for the diffusion of water molecules in a limited interlayer space. Therefore, the diffusion coefficient of water in the presence of $Na^+$ cations is greater. At high temperatures, the $Na^+$ hydration shell loses significantly more water molecules than $Cs^+$ ($Rb^+$) in their mixture. Therefore, with increasing temperature, the diffusion coefficient of water is greater in the solution with $Na^+$ than with $Cs^+$ or $Rb^+$.

Figure 3 shows the calculated graphs of the temperature dependence of the self-diffusion coefficients of cations in vermiculite containing two different interlayer counterions, for example, $9Na^+ + 3Cs^+$ and $6Na^+ + 3Ba^{2+}$. The data in Figure 3 allow comparing the changes in the diffusion coefficients with the addition of cations of alkali (Figure 3a) and alkaline earth (Figure 3b) metals. It can be seen from the figure that the diffusion rate of the $Na^+$ ion significantly decreases with the addition of another interlayer cation. Moreover, the larger the radius of the added ion is, the stronger is the effect on the diffusion of the $Na^+$ ion. The effect of alkaline earth metal ions is more vital than that of alkali metal ions. This may be due to cation competition.[49] At the same time, ions with a large radius and higher valence have great competitive advantages due to the ratio of the interaction energies of the cations with water molecules between the layers and with the charges on the surface of the mineral layer. However, the change in the diffusion coefficient of cations with increasing temperature is weakly expressed.

According to Zhang et al.,[5] temperature has little effect on the diffusion of cations in clays with poor hydration, and the effect of temperature becomes more significant with an increase in the degree of hydration. In highly hydrated clays, the effect of temperature is more significant than with weak hydration. In addition, the size and mass of the hydrated cation also affect the diffusion behavior of water and cations in the interlayer space of hydrated clays. Comparing the effect of temperature on the diffusion of water and ions between clay layers, it follows that the effect of temperature on the diffusion coefficient of water molecules is greater than that of ions.

Calculations show that the cations in the interlayer space of the clay are not evenly distributed but are grouped into layers. Depending on the structural features of the mineral, this distribution can be symmetric or asymmetric. In the model under study, Si atoms located in tetrahedra are replaced by Al only on one side of the clay layer. In such a structure, an uneven distribution of cations in the interlayer space is observed. Cations are more strongly adsorbed by the surface on one side of the layer containing a larger number of replaced atoms.[40] In this case, the concentration of charges of the tetrahedral sheet of the vermiculite layer, which determines the strength of ionic bonds, can also contribute to a slight change in the diffusion coefficient of cations with a change in temperature. Our results on the influence of the charge distribution over the basal surface on the adsorption of interlayer cations and the nonuniform distribution of sodium ions in the interlayer space do not contradict the data in the literature.[4,42]

It is known that water molecules form clusters, the size distribution of which depends on temperature.[50] The size of the hydration shell is proportional to the charge/cation size ratio, which determines the efficiency of the ion−dipole interaction. The charge/size value increases in the following


https://doi.org/10.1021/acsomega.1c06059
ACS Omega 2022, 7, 11596−11605

**Table 2. Calculated and Experimental Data on Diffusion Coefficients**

| particle | clay system from references | temperature, K | $D_O$, $m^2/s^a$ | $D_0$, $m^2/s^b$ | method | ref |
|---|---|---|---|---|---|---|
| water | Na-vermiculite, 3-layer hydrated | 285 | $5.83 \times 10^{-10}$ | $8.12 \times 10^{-11}$ | MD | 51 |
| | two-dimensional Na-vermiculite, 2-layer hydrated | 265 | | $5.5 \times 10^{-10}$ | experiment | 52 |
| | two-dimensional Na-vermiculite, 2-layer hydrated | 300 | $8.64 \times 10^{-10}$ | $8.8 \times 10^{-10}$ | experiment | 52 |
| $Na^+$ | Na-vermiculite, 3-layer hydrated | 285 | $3.04 \times 10^{-11}$ | $2.25 \times 10^{-11}$ | MD | 51 |
| | Montana vermiculite, <2 $\mu$m | 293 | $3.98 \times 10^{-11}$ | $6.1 \times 10^{-13}$ | experiment | 53 |
| | Na/Ca-vermiculite, water-saturated conditions | 298 | $4.63 \times 10^{-11}$ | $3.7 \times 10^{-11}$ | MD | 2 |
| | Na-vermiculite, clay concentration 49.5% | 298 | $4.63 \times 10^{-11}$ | $5.11 \times 10^{-11}$ | experiment | 54 |
| $Ba^{2+}$ | vermiculite, 3.6 mm diameter | 298 | $8.725 \times 10^{-12}$ | $(1.3–4.5) \times 10^{-11}$ | experiment | 53 |
| | Montana vermiculite, $C_{Ba}$ 0.1 equiv/1 | 344.65 | $1.32 \times 10^{-11}$ | $2.96 \times 10^{-11}$ | experiment | 55 |

$^a D_o$: the result of our calculations by using the MD method. $^b D_0$: from references.

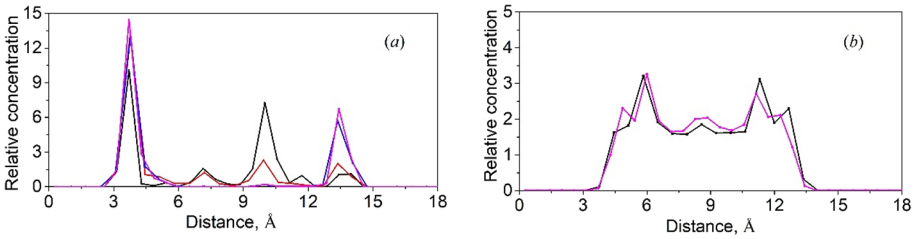


**Figure 4.** Density profile of cations (a) and water (b) in Na-vermiculite between clay layers for temperatures of 275 K (black), 300 K (red), 350 K (blue), and 400 K (pink).

order: $Cs^+$ (0.59), $Rb^+$ (0.67), $Na^+$ (1.05), $Ba^{2+}$ (1.48), and $Mg^{2+}$ (3.08). As the temperature rises, larger clusters are destroyed and the absolute concentration of small water clusters increases, and the number of water molecules in the hydration shell of the cation also decreases.

The diffusion coefficients of $Cs^+$, $Rb^+$, $Mg^{2+}$, and $Ba^{2+}$ ions through the vermiculite mineral, which simultaneously contains the $Na^+$ cation, nonmonotonically increase in the temperature range of 275–425 K by a small amount. This can be explained by the destruction of the hydration shell during heating, which represents a potential well, which leads to an increase in the mobility. In this case, the distance between the cation and the charges on the layer surface also decreases, reducing the cations' mobility. Due to the difference in ionic radii, the cations approach the layer surface at different distances. The diffusion coefficient of $Na^+$ is greater than that of $Cs^+$, $Rb^+$, $Mg^{2+}$, and $Ba^{2+}$ due to its smaller mass. It is possible that a decrease in the cluster size increases the role of the hydration shell in the formation of a potential well due to the partial polarization of nearby water dimers.

The diffusion coefficient of $Na^+$, in the absence of other cations, fluctuates around the value of $4 \times 10^{-11}$ $m^2/s$, with a tendency to decrease upon heating. This may be due to a decrease in the effect of the hydration shell and concentration of $Na^+$ near the layer surface and an increase in the force of interaction of charges, as well as an increase in the number of collisions with water molecules, which transfer momentum mainly toward the layer surface.

In the presence of $Rb^+$, $Na^+$ ions are located closer to the layer surface than in the presence of $Cs^+$, $Ba^{2+}$, and $Mg^{2+}$ or in a one-component solution. This trend intensifies with increasing temperatures. Therefore, in a mixture with $Rb^+$, the diffusion coefficient of $Na^+$ tends to decrease upon heating.

The diffusion coefficient of $Na^+$, mixed with $Cs^+$, $Rb^+$, $Mg^{2+}$, and $Ba^{2+}$, changes nonmonotonically upon heating from 275 to 425 K. At 373 K, there are maxima of the diffusion coefficient of $Na^+$ in a mixture with $Cs^+$ or $Ba^{2+}$. When heated above 373 K, the diffusion coefficient of $Na^+$ in the presence of $Cs^+$, $Ba^{2+}$, and $Mg^{2+}$ increases after a significant decrease. This trend is also seen in pure $Na^+$. At different temperatures, there is also a different ratio of the diffusion coefficients of $Na^+$, which is in a mixture with other cations. For example, at 275 K, the $Na^+$ diffusion coefficient increases in the following order in a mixture with $Ba^{2+}$, $Rb^+$, $Mg^{2+}$, and $Cs^+$. At 350 K, the $Na^+$ diffusion coefficient increases in a mixture with $Rb^+$, $Mg^{2+}$, $Cs^+$, and $Ba^{2+}$.

It is known that, in a condensed state, the energy of thermal vibrations of individual particles fluctuates. Cations in the interlayer space of clay move to another point if the energy of their thermal vibrations exceeds the value of the potential well. In the case considered in the article, the probability of a collision of a cation with the hydration shell of another cation is high. If during a collision the total energy of two cations exceeds the depth of the second potential well, then the second cation can be replaced by the first one.

The probability of moving the first cation is the maximum if the energy fluctuations of the first and second cations occur after a time equal to the time of flight of the first cation from its first position to the second cation. This time also depends on the temperature. For example, the maximum diffusion coefficient of $Na^+$ mixed with $Cs^+$ or $Ba^{2+}$ appears at a temperature of 375 K. In other cases, such a "resonance" is not observed since it is outside the considered temperatures.

Our calculated data do not contradict the experimental data of other authors (see Table 2). Some differences in the data are associated with the difference in the conditions for the experiments and calculations.

**3.2. Distribution of Different Cations among Clay Layers.** Heating enhances the thermal movement of atoms and molecules, which leads to an increase in the diffusion coefficient. For compositions of vermiculite and cations of alkali and alkaline earth metals, this regularity is poorly fulfilled. Therefore, we simulated the structural features of the interaction of cations and water molecules in the interlayer


https://doi.org/10.1021/acsomega.1c06059
ACS Omega 2022, 7, 11596–11605

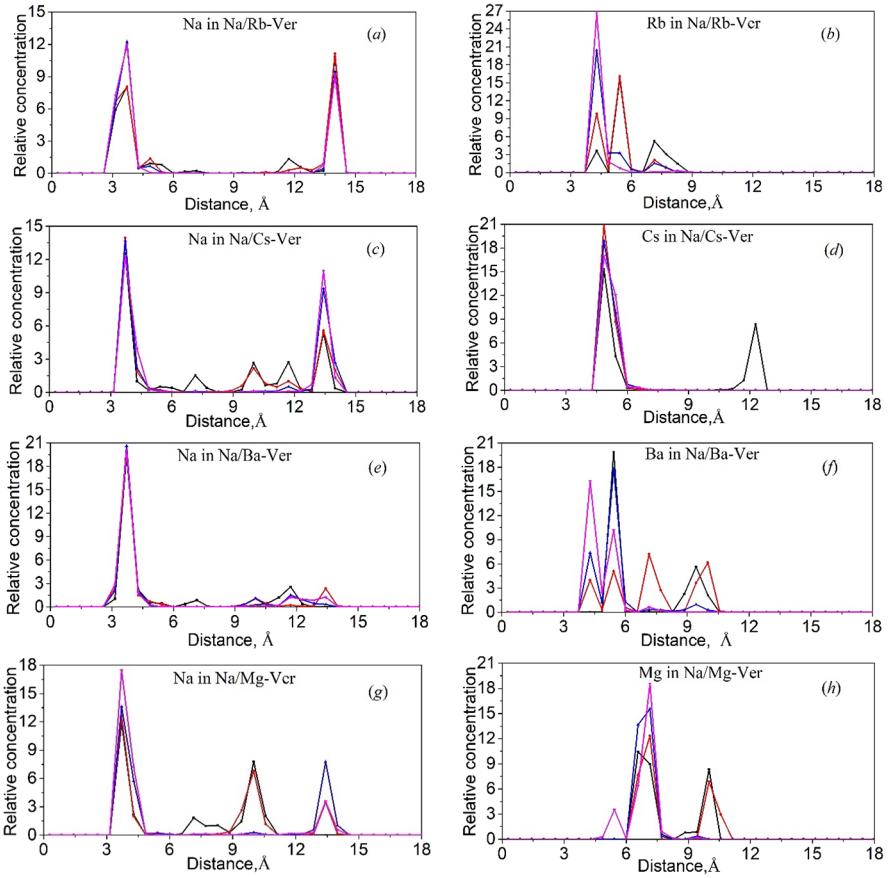


**Figure 5.** Density profile of (a) $Na^+$ in Na/Rb-vermiculite, (b) $Rb^+$ in Na/Rb-vermiculite, (c) $Na^+$ in Na/Cs-vermiculite, (d) $Cs^+$ in Na/Cs-vermiculite, (e) $Na^+$ in Na/Ba-vermiculite, (f) $Ba^{2+}$ in Na/Ba-vermiculite, (g) $Na^+$ in Na/Mg-vermiculite, and (h) $Mg^{2+}$ in Na/Mg-vermiculite for different temperatures of 275 K (black), 300 K (red), 350 K (blue), and 425 K (pink).

space with clay layers. At the same time, the possibility of dissociation of water molecules was neglected.

To gain a deeper understanding of the interaction of various cations with the surface of the clay layer, we calculated the distribution of various cations in the interlayer region perpendicular to the basal surface of the clay layer. As can be seen from Figure 4a, at a temperature of 275 K, interlayer cations of $Na^+$ are concentrated at distances 3.71, 7.14, 9.99, 11.71, and 13.42 Å from the center of the octahedral sheet of the layer. In this case, the direction of the coordinate axis is oriented from the surface of one layer containing Al to the surface of another layer in which Si atoms are not replaced by Al. As the temperature rises above 350 K, the concentration of cations is observed near the surfaces of clay layers. Asymmetry in the distribution of cations arises due to the fact that two layers of clay with different surface charges interact with each other. The distribution of these cations determines the energy balance in vermiculite−cation and water−cation interactions. Five peaks at 275 K indicate that the interaction of the cation with water molecules is stronger than the interaction of the cation with the vermiculite surface.[56] As the temperature rises, a decrease in the hydration of cations is observed. Therefore, there is a transition from the adsorption of outer sphere surface complexes, which retain their coordinated shell of water molecules, to the adsorption of inner sphere surface complexes.[41] This means that as the temperature rises, there is a tendency for cations to concentrate near the surface of the clay layer. In inner sphere surface complexes, cations interact directly with the clay surface. Figure 4b shows the distribution curves of the concentration of water molecules at two temperatures. It can be seen that the third peak, formed in the middle, is more pronounced at 400 K and water molecules are more clearly grouped into three layers. This may be due to the fact that an increase in temperature leads to an increase in the number of free water molecules. At the same time, a larger number of water molecules are involved in the formation of the water concentration profile between the clay layers.

Asymmetry in the distribution of cations between clay layers is also observed in the presence of two ions simultaneously (see Figure 5). Figure 5 follows that one side of the clay layer more strongly attracts cations due to the uneven distribution of surface charges as a result of asymmetry in the relative amounts of Al replacing Si in two adjacent clay layers. Cations are more concentrated on the surface of tetrahedrons (tetrahedral sheet) with high aluminum content.[40] At low temperatures (for example, at 275 K), the layered distribution of $Na^+$ ions is less pronounced. At a temperature of 275 K, $Na^+$ ions are strongly adsorbed on the upper and lower surfaces of the clay layer. At temperatures above 350 K, the interlayer distribution in vermiculite is more ordered, with a general preference for adsorption on the surface of the tetrahedral sheet and an almost complete absence of ions in the middle between the clay layers.

Two peaks are observed after adding the $Rb^+$ ion for the $Na^+$ ion located at distances 3.71 and 13.99 Å. The addition of other cations does not cause such a change in the distribution



https://doi.org/10.1021/acsomega.1c06059
ACS Omega 2022, 7, 11596−11605

of the $Na^+$ ion at both 3.71 and 13.42 Å, which agrees with the data in the presence of only one ion $Na^+$, considered in the previous section. This may mean that the addition of the $Rb^+$ ion leads to the closer binding of the $Na^+$ ion with the tetrahedral structure compared to other ions. The $Cs^+$ ion is more strongly attracted to the layer surface than the $Na^+$ ion. With an increase in temperature above 325 K, the forces of attraction of $Cs^+$ and $Na^+$ ions with clay become equal.

With increasing temperature, the vibrational motion of atoms increases. Therefore, the degree of hydration of cations decreases. The predominant arrangement of $Ba^{2+}$ ions at low temperatures in the middle region between the clay layers leads to the fact that $Na^+$ ions are repelled from them and are more strongly attracted to the surface of the clay layer. As the temperature rises, $Ba^{2+}$ ions are also localized at the surface of the tetrahedral sheet. $Mg^{2+}$ ions, due to their smaller ionic radius (0.65 Å), are more hydrated than $Na^+$ ions (0.95 Å). At the same time, $Mg^{2+}$ ions cannot squeeze out $Na^+$ ions from the surface of the clay layer. Therefore, $Mg^{2+}$ is always located in the middle between the clay layers.

Hydrogen atoms of water molecules, which have a small positive charge, are attracted to the negative charge on the surface of the clay. Therefore, the hydrogen atoms of free water molecules are oriented to the clay surface. The outer surface of the vermiculite clay layer has a large negative charge and attracts all positively charged ions to the surface, including into the voids of the tetrahedral layer. $Na^+$ ions are more likely to be in the cavities between atoms forming the hexagonal structures of the tetrahedral sheet than other ions due to their minimal radius and stronger attraction.[57] On the contrary, $Mg^{2+}$ ions, which form a hydration shell with a large radius, are often located in the middle between the layers and do not compete with $Na^+$ ions. A diagram of two projections of the most probable spatial arrangement of $Na^+$ ions is shown in Figure 6.

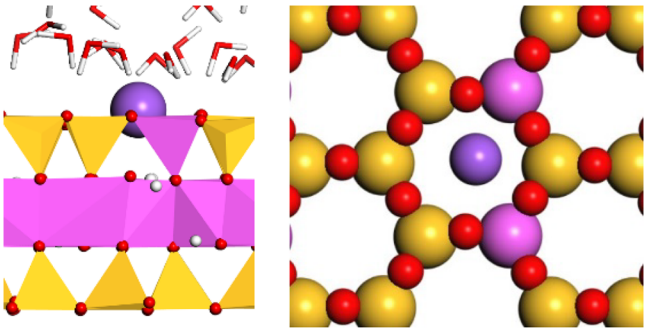


**Figure 6.** The projections diagrams of the cation relative to the surface of white mica: (a) side view and (b) top view.

**3.3. Interaction between Interlayer Cations and Water Molecules.** The importance of the hydration shells of cations for the temperature dependence of the diffusion coefficients is shown above. The hydration shell of cations can be characterized by a radial distribution function (RDF). Figure 7 shows the RDF curves for $Na^+$ in Na-vermiculite at temperatures of 275 and 425 K. It can be seen that the position of the first peak is retained at a distance of 2.35 Å in the curves at 275 and 425 K due to the interaction of $Na^+$ with the oxygen atom of water molecules ($O_w$). The distance between $Na^+$ and water oxygen in the first layer of the hydration shell does not change significantly. The second peak is shifted from 4.73 to 5.03 Å. This means that the second hydration shell increases slightly with increasing temperature. It is obvious that the height of the peak g(r) decreases in all cases as the temperature increases. Figure 7b shows the RDF for interaction with oxygen atoms on the clay surface ($O_s$). The RDF peak height increases significantly at 425 K. This confirms that with an increase in temperature, interlayer cations interact more with the surface of the clay layer than with water. However, a change in the temperature of the interlayer region does not lead to a significant change in the position of ions relative to the surface of the layer.

General RDF regularities are retained when a part of the $Na^+$ counterions is replaced by ions of other elements. Figure 8 shows the RDF curves for Na/Cs-vermiculite. The calculation results for vermiculite containing 75% $Na^+$ and 25% $Cs^+$, in comparison with the data for vermiculite with 100% $Na^+$, are shown in Figures 7a and 8a. When some interlayer $Na^+$ ions are replaced by $Cs^+$, the hydration shell of $Na^+$ decreases due to competition between the cations. This is indicated by an increase in the height of the RDF peak in Figure 8b relative to Figure 7b, which leads to an increase in the interaction of $Na^+$ with the surface of the clay layer. For the data in Figure 8c,d, in the interlayer space, 25% of $Na^+$ ions are replaced by $Cs^+$. The height of the RDF peak decreases slightly upon heating. This is due to the fact that $Cs^+$ ions are located farther from the layer surface than $Na^+$. Therefore, $Cs^+$ cannot displace $Na^+$ on the clay surface, especially at high temperatures.

For the monovalent ions considered above, the following regularities are observed. With increasing temperature, the fraction of oxygen atoms on the layer surface interacting with $Cs^+$ decreases, and for $Na^+$ ions, it increases. However, the distances between the cation ($Na^+$ or $Cs^+$) and the surface of the vermiculite layer do not change, as well as to the water molecules in their hydration shell.

Replacing monovalent cations with divalent ions of alkaline earth elements can lead to a change in the charge of the system. To keep the crystals of vermiculite clay as a whole electrically neutral, two $Na^+$ ions were replaced by one alkaline earth ion $Ba^{2+}$. Figure 9 shows the RDF curves for Na/Ba-

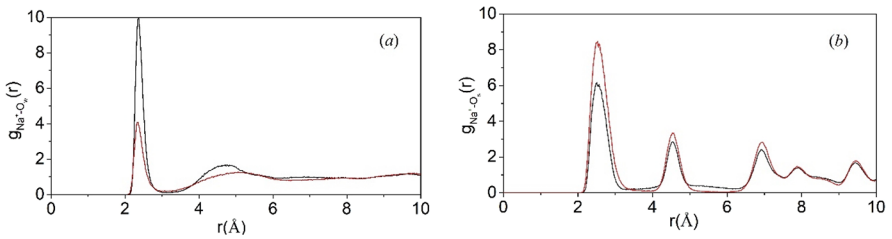


**Figure 7.** Radial distribution functions for Na-$O_W$ (a) and Na-$O_S$ (b) for Na-vermiculite in temperatures of 275 K (black) and 425 K (red).



https://doi.org/10.1021/acsomega.1c06059
ACS Omega 2022, 7, 11596−11605

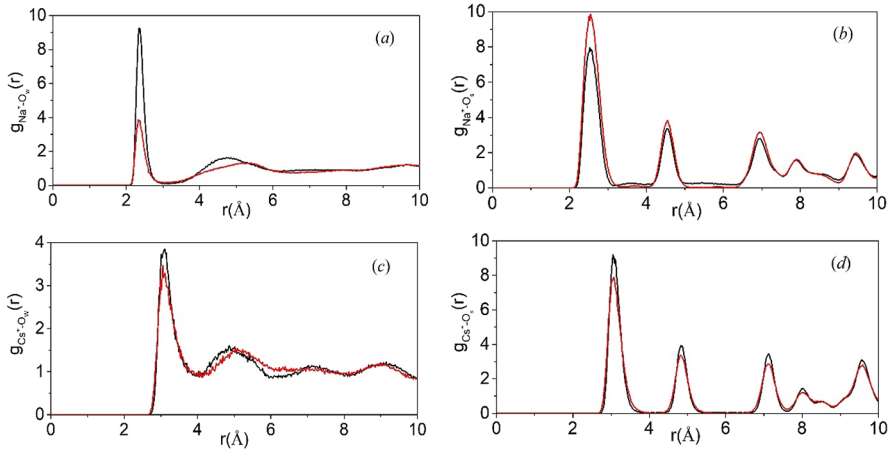


**Figure 8.** Radial distribution functions for Na-$O_w$ (a), Na-$O_S$ (b), Cs-$O_w$ (c), and Cs-$O_S$ (d) for Na/Cs-vermiculite in temperatures of 275 K (black) and 425 K (red).

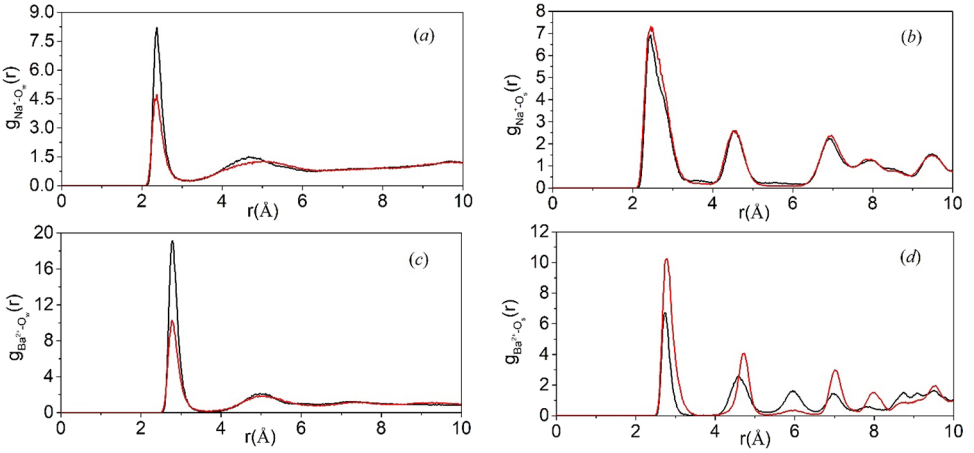


**Figure 9.** Radial distribution functions for Na-$O_w$ (a), Na-$O_S$ (b), Ba-$O_w$ (c), and Ba-$O_S$ (d) for Na/Ba-vermiculite in temperatures of 275 K (black) and 425 K (red).

vermiculite. Comparison of Figure 9a with Figures 7a and 8a shows that, at 425 K, the density of water molecules around $Na^+$ ions increases after the addition of $Ba^{2+}$. In this case, the size of the second layer of the $Na^+$ hydration shell always increases.

In Figure 9b, it can be seen that, when heated to 425 K, $Na^+$ ions slightly move away from the surface of the clay layer. In this case, the number of oxygen atoms on the surface of the clay layer, interacting with the cation, remains almost unchanged. In contrast, in Figure 9d, the Ba-$O_s$ peak near the vermiculite surface is higher at 425 K. This clearly indicates that the $Ba^{2+}$ ions interact with a larger number of oxygen atoms on the clay layer surface than the $Na^+$ ion. However, upon heating, the $Ba^{2+}$ ions are displaced from a distance of 2.73 Å by a slightly greater distance of 2.77 Å relative to the surface of the clay layer.

Comparison of the calculation results for Na-vermiculite, when replacing part of the cations with ions of other alkaline and alkaline earth elements, shows a different effect of different cations on the hydration of $Na^+$ ions and their adsorption on the surface of the clay layer. Compared to alkali metal ions, alkaline earth metal ions have great competitive advantages in terms of adsorption on surfaces at different temperatures. Due to the strong adsorption of alkaline earth metal ions on the hexagonal ring, neither replacement of ions nor an increase in temperature significantly changes the position of $Na^+$ or $Ba^{2+}$ cations near the surface of the layer. Also, a decrease in the total number of cations when some of the $Na^+$ ions are replaced by alkaline earth metal ions, for example, $Ba^{2+}$, does not have a strong effect on the temperature dependence of the diffusion coefficient of $Na^+$ ions.

## 4. SUMMARY

The MD method was used to model vermiculite containing different cations by partial substitution of $Na^+$ ions between clay layers. The diffusion coefficient was determined by studying the kinetic regularities of the movement of various interlayer cations at different temperatures. It was found that the effect of temperature on the diffusion of water is much greater than that on the diffusion of cations. In low-hydrated clays, temperature does not significantly affect the diffusion coefficient of water and cations. The size and mass of the hydrated cation strongly influence its diffusion and adsorption behavior on the surface of the clay layer.

The density distribution and structure of RDF for the adsorption of $Na^+$ ions on a vermiculite clay layer were studied by the MD method. Calculations were carried out for clay in which the interlayer $Na^+$ cations are partially replaced by $Rb^+$, $Cs^+$, $Mg^{2+}$, and $Ba^{2+}$ ions. It is shown that the effect of different ions on the interlayer $Na^+$ ions is significantly different at


https://doi.org/10.1021/acsomega.1c06059
ACS Omega 2022, 7, 11596−11605

different temperatures. Alkali metal ions have a larger ionic radius than $Na^+$. At the same time, their force of interaction with charges on the surface of the clay layer is less than that of $Na^+$ ions. Therefore, $Na^+$ ions are localized at the surface. Alkaline earth metal cations are in the middle region between clay layers due to their higher charge and stronger hydration.

## AUTHOR INFORMATION


### Corresponding Author

**Cailun Wang** − *Division for Nuclear-Fuel Cycle, Tomsk Polytechnic University, Tomsk 634050, Russian Federation;* orcid.org/0000-0003-2887-6672; Phone: +79234157599; Email: caylun1224@gmail.com

### Authors

**Vyacheslav Fedorovich Myshkin** − *Division for Nuclear-Fuel Cycle, Tomsk Polytechnic University, Tomsk 634050, Russian Federation*

**Valeriy Alekseevich Khan** − *Division for Nuclear-Fuel Cycle, Tomsk Polytechnic University, Tomsk 634050, Russian Federation; Zuev Institute of Atmospheric Optics of the Siberian Branch of the RAS, Tomsk 634055, Russian Federation*

**Andrew Dmitrievich Poberezhnikov** − *Division for Nuclear-Fuel Cycle, Tomsk Polytechnic University, Tomsk 634050, Russian Federation*

**Alexander Petrovich Baraban** − *Department of Solid-State Electronics, Saint-Petersburg State University, St. Petersburg 198504, Russian Federation*

Complete contact information is available at: https://pubs.acs.org/10.1021/acsomega.1c06059


### Notes

The authors declare no competing financial interest.

## ACKNOWLEDGMENTS

The research was carried out within the framework of the Program for Enhancing Competitiveness of National Research Tomsk Polytechnic University. The authors would like to thank Prof. Baraban from Saint-Petersburg State University for providing the software Materials Studio used in this study. Finally, the authors warmly acknowledge three anonymous reviewers and editor (Deqing Zhang) for their many suggestions, which drastically improved the results and the clarity of the manuscript.

## REFERENCES


(1) González Sánchez, F.; Van Loon, L. R.; Gimmi, T.; Jakob, A.; Glaus, M. A.; Diamond, L. W. Self-diffusion of water and its dependence on temperature and ionic strength in highly compacted montmorillonite, illite and kaolinite. *Appl. Geochem.* **2008**, *23*, 3840−3851.

(2) Tertre, E.; Delville, A.; Prêt, D.; Hubert, F.; Ferrage, E. Cation diffusion in the interlayer space of swelling clay minerals − A combined macroscopic and microscopic study. *Geochim. Cosmochim. Acta* **2015**, *149*, 251−267.

(3) Teich-McGoldrick, S. L.; Greathouse, J. A.; Jové-Colón, C. F.; Cygan, R. T. Swelling Properties of Montmorillonite and Beidellite Clay Minerals from Molecular Simulation: Comparison of Temperature, Interlayer Cation, and Charge Location Effects. *J. Phys. Chem. C* **2015**, *119*, 20880−20891.

(4) Sun, L.; Ling, C. Y.; Lavikainen, L. P.; Hirvi, J. T.; Kasa, S.; Pakkanen, T. A. Influence of layer charge and charge location on the swelling pressure of dioctahedral smectites. *Chem. Phys.* **2016**, *473*, 40−45.

(5) Zhang, X.; Yi, H.; Zhao, Y.; Min, F.; Song, S. Study on the differences of Na- and Ca-montmorillonites in crystalline swelling regime through molecular dynamics simulation. *Adv. Powder Technol.* **2016**, *27*, 779−785.

(6) Li, H.; Song, S.; Dong, X.; Min, F.; Zhao, Y.; Peng, C.; Nahmad, Y. Molecular Dynamics Study of Crystalline Swelling of Montmorillonite as Affected by Interlayer Cation Hydration. *JOM* **2018**, *70*, 479−484.

(7) Xu, J.; Camara, M.; Liu, J.; Peng, L.; Zhang, R.; Ding, T. Molecular dynamics study of the swelling patterns of Na/Cs-, Na/Mg-montmorillonites and hydration of interlayer cations. *Mol. Simul.* **2017**, *43*, 575−589.

(8) Peng, J.; Yi, H.; Song, S.; Zhan, W.; Zhao, Y. Driving force for the swelling of montmorillonite as affected by surface charge and exchangeable cations: A molecular dynamic study. *Results Phys.* **2019**, *12*, 113−117.

(9) Missana, T.; Alonso, U.; Fernández, A. M.; García-Gutiérrez, M. Colloidal properties of different smectite clays: Significance for the bentonite barrier erosion and radionuclide transport in radioactive waste repositories. *Appl. Geochem.* **2018**, *97*, 157−166.

(10) Grambow, B. Geological Disposal of Radioactive Waste in Clay. *Elements* **2016**, *12*, 239−245.

(11) Sellin, P.; Leupin, O. X. The Use of Clay as an Engineered Barrier in Radioactive-Waste Management − A Review. *Clays Clay Miner.* **2013**, *61*, 477−498.

(12) Bourg, I. C.; Sposito, G.; Bourg, A. C. Modeling cation diffusion in compacted water-saturated sodium bentonite at low ionic strength. *Environ. Sci. Technol.* **2007**, *41*, 8118−8122.

(13) Do, N. Y.; Lee, S. R. Temperature effect on migration of Zn and Cd through natural clay. *Environ. Monit. Assess.* **2006**, *118*, 267−291.

(14) Dultz, S.; Riebe, B.; Bunnenberg, C. Temperature effects on iodine adsorption on organo-clay minerals. *Appl. Clay Sci.* **2005**, *28*, 17−30.

(15) Greathouse, J. A.; Cygan, R. T.; Fredrich, J. T.; Jerauld, G. R. Adsorption of Aqueous Crude Oil Components on the Basal Surfaces of Clay Minerals: Molecular Simulations Including Salinity and Temperature Effects. *J. Phys. Chem. C* **2017**, *121*, 22773−22786.

(16) Greathouse, J. A.; Hart, D. B.; Bowers, G. M.; Kirkpatrick, R. J.; Cygan, R. T. Molecular Simulation of Structure and Diffusion at Smectite−Water Interfaces: Using Expanded Clay Interlayers as Model Nanopores. *J. Phys. Chem. C* **2015**, *119*, 17126−17136.

(17) Marry, V.; Dubois, E.; Malikova, N.; Durand-Vidal, S.; Longeville, S.; Breu, J. Water dynamics in hectorite clays: influence of temperature studied by coupling neutron spin echo and molecular dynamics. *Environ. Sci. Technol.* **2011**, *45*, 2850−2855.

(18) Mon, E. E.; Hamamoto, S.; Kawamoto, K.; Komatsu, T.; Moldrup, P. Temperature effects on solute diffusion and adsorption in differently compacted kaolin clay. *Environ. Earth Sci.* **2016**, *75*, 1−9.

(19) Romero, E.; Gens, A.; Lloret, A. Temperature effects on the hydraulic behaviour of an unsaturated clay. *Geotech. Geol. Eng.* **2001**, *19*, 311−332.

(20) Sui, H.; Yao, J.; Zhang, L. Molecular Simulation of Shale Gas Adsorption and Diffusion in Clay Nanopores. *Computation* **2015**, *3*, 687−700.

(21) Tian, H.; Wei, C.; Yan, R. Thermal and saline effect on mineral-water interactions in compacted clays: A NMR-based study. *Appl. Clay Sci.* **2019**, *170*, 106−113.

(22) Xie, S.; Wen, Z.; Zhan, H.; Jin, M. An Experimental Study on the Adsorption and Desorption of Cu(II) in Silty Clay. *Geofluids* **2018**, *2018*, 1−12.

(23) Zheng, Y.; Zaoui, A. Temperature effects on the diffusion of water and monovalent counterions in the hydrated montmorillonite. *Phys. A* **2013**, *392*, 5994−6001.

(24) Rongwei, S.; Tsukahara, T. Effect of Cations on Interlayer Water Dynamics in Cation-Exchanged Montmorillonites Studied by

Nuclear Magnetic Resonance and X-ray Diffraction Techniques. *ACS Earth Space Chem.* **2020**, *4*, 535−544.
(25) Cygan, R. T.; Liang, J.-J.; Kalinichev, A. G. Molecular Models of Hydroxide, Oxyhydroxide, and Clay Phases and the Development of a General Force Field. *J. Phys. Chem. B* **2004**, *108*, 1255−1266.
(26) Marty, N. C. M.; Grangeon, S.; Lassin, A.; Madé, B.; Blanc, P.; Lanson, B. A quantitative and mechanistic model for the coupling between chemistry and clay hydration. *Geochim. Cosmochim. Acta* **2020**, *283*, 124−135.
(27) Reddy, U. V.; Bowers, G. M.; Loganathan, N.; Bowden, M.; Yazaydin, A. O.; Kirkpatrick, R. J. Water Structure and Dynamics in Smectites: X-ray Diffraction and 2H NMR Spectroscopy of Mg−, Ca−, Sr−, Na−, Cs−, and Pb−Hectorite. *J. Phys. Chem. C* **2016**, *120*, 8863−8876.
(28) Mooney, R. W.; Keenan, A. G.; Wood, L. A. Adsorption of water vapor by montmorillonite. II. Effect of exchangeable ions and lattice swelling as measured by X-ray diffraction. *J. Am. Chem. Soc.* **1952**, *74*, 1371−1374.
(29) Boek, E. S.; Coveney, P. V.; Skipper, N. T. Monte Carlo molecular modeling studies of hydrated Li-, Na-, and K-smectites: Understanding the role of potassium as a clay swelling inhibitor. *J. Am. Chem. Soc.* **1995**, *117*, 12608−12617.
(30) Liu, X.; Lu, X.; Wang, R.; Zhou, H. Effects of layer-charge distribution on the thermodynamic and microscopic properties of Cs-smectite. *Geochim. Cosmochim. Acta* **2008**, *72*, 1837−1847.
(31) Camara, M.; Xu, J.; Wang, X.; Zhang, J.; Chen, Z.; Li, X. Molecular dynamics simulation of hydrated Na-montmorillonite with inorganic salts addition at high temperature and high pressure. *Appl. Clay Sci.* **2017**, *146*, 206−215.
(32) Li, X.; Zhu, C.; Jia, Z.; Yang, G. Confinement effects and mechanistic aspects for montmorillonite nanopores. *J. Colloid Interface Sci.* **2018**, *523*, 18−26.
(33) Malikova, N.; Cadéne, A.; Marry, V.; Dubois, E.; Turq, P.; Zanotti, J. M.; Longeville, S. Diffusion of water in clays − microscopic simulation and neutron scattering. *Chem. Phys.* **2005**, *317*, 226−235.
(34) Xu, D. Adsorption of Pb(II) from aqueous solution to MX-80 bentonite: Effect of pH, ionic strength, foreign ions and temperature. *Appl. Clay Sci.* **2008**, *41*, 37−46.
(35) Hongxia, Z.; Xiaoyun, W.; Honghong, L.; Tianshe, T.; Wangsuo, W. Adsorption behavior of Th(IV) onto illite: Effect of contact time, pH value, ionic strength, humic acid and temperature. *Appl. Clay Sci.* **2016**, *127-128*, 35−43.
(36) Komadel, P.; Madejová, J.; Bujdák, J. Preparation and properties of reduced-charge smectites − a review. *Clays Clay Miner.* **2005**, *53*, 313−334.
(37) Michels, L.; da Fonseca, C. L. S.; Méheust, Y.; Altoé, M. A. S.; dos Santos, E. C.; Grassi, G.; Droppa, R.; Knudsen, K. D.; Cavalcanti, L. P.; Hunvik, K. W. B.; Fossum, J. O.; da Silva, G. J.; Bordallo, H. N. The Impact of Thermal History on Water Adsorption in a Synthetic Nanolayered Silicate with Intercalated Li+ or Na+. *J. Phys. Chem. C* **2020**, *124*, 24690−24703.
(38) Zhu, R.; Chen, Q.; Zhu, R.; Xu, Y.; Ge, F.; Zhu, J.; He, H. Sequestration of heavy metal cations on montmorillonite by thermal treatment. *Appl. Clay Sci.* **2015**, *107*, 90−97.
(39) Wyckoff, R. W. G. *Crystal structures*; New York [etc.] : Interscience, 1964; Vol. *2*, 2nd ed, pp 1−588.
(40) Zaunbrecher, L. K.; Cygan, R. T.; Elliott, W. C. Molecular Models of Cesium and Rubidium Adsorption on Weathered Micaceous Minerals. *J. Phys. Chem. A* **2015**, *119*, 5691−5700.
(41) Skipper, N. T.; Chang, F. R. C.; Sposito, G. Monte Carlo Simulation of Interlayer Molecular Structure in Swelling Clay Minerals. *1. Methodology. Clays Clay Miner.* **1995**, *43*, 285−293.
(42) Ngouana, W. B. F.; Kalinichev, A. G. Structural Arrangements of Isomorphic Substitutions in Smectites: Molecular Simulation of the Swelling Properties, Interlayer Structure, and Dynamics of Hydrated Cs−Montmorillonite Revisited with New Clay Models. *J. Phys. Chem. C* **2014**, *118*, 12758−12773.
(43) Zheng, Y.; Zaoui, A.; Shahrour, I. A theoretical study of swelling and shrinking of hydrated Wyoming montmorillonite. *Appl. Clay Sci.* **2011**, *51*, 177−181.
(44) Suter, J. L.; Coveney, P. V.; Greenwell, H. C.; Thyveetil, M.-A. Large-Scale Molecular Dynamics Study of Montmorillonite Clay: Emergence of Undulatory Fluctuations and Determination of Material Properties. *J. Phys. Chem. C* **2007**, *111*, 8248−8259.
(45) Tesson, S.; Salanne, M.; Rotenberg, B.; Tazi, S.; Marry, V. Classical Polarizable Force Field for Clays: Pyrophyllite and Talc. *The Journal of Physical Chemistry C* **2016**, *120*, 3749−3758.
(46) Dzene, L.; Ferrage, E.; Hubert, F.; Delville, A.; Tertre, E. Experimental evidence of the contrasting reactivity of external vs. interlayer adsorption sites on swelling clay minerals: The case of Sr2+−for-Ca2+ exchange in vermiculite. *Appl. Clay Sci.* **2016**, *132-133*, 205−215.
(47) Tertre, E.; Dazas, B.; Asaad, A.; Ferrage, E.; Grégoire, B.; Hubert, F.; Delville, A.; Delay, F. Connecting molecular simulations and laboratory experiments for the study of time-resolved cation-exchange process in the interlayer of swelling clay minerals. *Appl. Clay Sci.* **2021**, *200*, 105913.
(48) Yang, Y.; Narayanan Nair, A. K.; Sun, S. Layer Charge Effects on Adsorption and Diffusion of Water and Ions in Interlayers and on External Surfaces of Montmorillonite. *ACS Earth Space Chem.* **2019**, *3*, 2635−2645.
(49) Skipper, N. T.; Refson, K.; McConnell, J. D. C. Computer simulation of interlayer water in 2:1 clays. *J. Chem. Phys.* **1991**, *94*, 7434−7445.
(50) Hagler, A. T.; Scheraga, H. A.; Nemethy, G. Structure of liquid Water. Statistical Thermodynamic Theory. *J. Phys. Chem. A* **1972**, *76*, 3229−3243.
(51) Yang, W.; Zheng, Y.; Zaoui, A. Swelling and diffusion behaviour of Na-vermiculite at different hydrated states. *Solid State Ionics* **2015**, *282*, 13−17.
(52) Swenson, J.; Bergman, R.; Howells, W. S. Quasielastic neutron scattering of two-dimensional water in a vermiculite clay. *J. Chem. Phys.* **2000**, *113*, 2873−2879.
(53) Nye, P. H. Diffusion of ions and uncharged solutes in soils and soil clays. *Adv. Agron.* **1980**, *31*, 225−272.
(54) Lai, T. M.; Mortland, M. M. Diffusion of Ions in Bentonite and Vermiculite. *Soil Sci. Soc. Am. J.* **1961**, *25*, 353−357.
(55) Lutze, W.; Miekeley, N. Ion-exchange kinetics in vermiculite. *J. Phys. Chem. A* **1971**, *75*, 2484−2488.
(56) Sakuma, H.; Kawamura, K. Structure and dynamics of water on Li+−, Na+−, K+-, Cs+−, H3O+-exchanged muscovite surfaces: A molecular dynamics study. *Geochim. Cosmochim. Acta* **2011**, *75*, 63−81.
(57) Bourg, I. C.; Sposito, G. Molecular dynamics simulations of the electrical double layer on smectite surfaces contacting concentrated mixed electrolyte (NaCl−CaCl2) solutions. *J. Colloid Interface Sci.* **2011**, *360*, 701−715.


https://doi.org/10.1021/acsomega.1c06059
*ACS Omega* 2022, 7, 11596−11605